Journal of Inclusion Phenomena and Molecular Recognition in Chemistry **28:** 271–285, 1997.

Phase Diagram of the Xe–H_2O System up to 15 kbar

YU A. DYADIN, E.G. LARIONOV, D.S. MIRINSKIJ, T.V. MIKINA, E. YA ALADKO and L.I. STAROSTINA
Institute of Inorganic Chemistry, Russian Academy of Sciences, Siberian Branch, 630090 Novosibirsk, Russia.

(Received: 19 March 1996; in final form: 6 December 1996)

Abstract. The phase equilibria in the Xe–H_2O system have been studied by the DTA technique under hydrostatic pressures up to 15 000 bar in a temperature range from −25 °C to 100 °C. We have shown that the cubic structure **I** xenon hydrate forming at ambient pressure does not undergo any phase transitions under the conditions studied. The temperature of its decomposition into water solution and gas (fluid) increases from 27 °C at 25 bar to 78.2 °C at 6150 bar. At higher pressures the hydrate decomposes into water solution and solid xenon. In the temperature range from 6800 to 9500 bar the decomposition temperature (79.0–79.5 °C) is practically independent of pressure, while further pressure increase results in a slow decrease to 67 °C at 15 000 bar.

Key words: Xenon hydrate, high pressure, phase diagram, clathrate hydrate, gas hydrate.

1. Introduction

The xenon hydrate $Xe{\cdot}6H_2O$ was first discovered in 1925 by Forcrand [1] who was studying phase equilibria in the Xe–H_2O system at pressures up to 17.2 bar. Two years earlier he had discovered a similar hydrate in the Kr–H_2O system and reported data on its decomposition at pressures up to 47.8 bar [2]. Krypton and xenon hexadeuterates were reported in reference [3]. Elegant experiments on isomorphous coprecipitation of radon hydrate with sulfurous gas and hydrogen sulfide hydrates (for known reasons it is not possible to obtain radon in quantities sufficient for the formation of the phase of its own hydrate) led Nikitin [4] to conclude that radon formed a hexahydrate of intermediate stability. However, the first compound of a noble gas, $Ar{\cdot}6H_2O$, was discovered in 1896 by Villard [5], only a little more than a year after Ramsay and Rayleigh discovered argon. Now it is well known that all of these hydrates are clathrates [6, 7]. Xenon hydrate has cubic structure **I** (*CS-I*) [6] while krypton and argon hydrates, contrary to what was believed for a long time [1][6], are of cubic structure **II** (*CS-II*) [7] where the large cavity and many of the small cavities are occupied by the guest molecules, giving a composition close to $M{\cdot}6H_2O$. Helium [10,11] as well as hydrogen [12,13] does not form classic clathrate hydrates but dissolves in the ices Ih and II. The hydrogen system has been studied at very high pressures and hydrogen has been shown to form clathrate $H_2{\cdot}H_2O$ hydrate on the ice Ic basis at pressures higher than 23 000 bar at room temperature. It is stable at least at pressures up to 300 000 bar [12].

The guest molecules in water – 'heavy' noble gas systems are obviously very valuable as models for the study of clathrate gas hydrates under ordinary conditions and especially at high pressures. The physical chemistry of gaseous hydrates has recently been attracting increasing attention from researchers due to the discovery of practically inexhaustible natural gas deposits (in the form of clathrate hydrates) in the interior of the Earth [14] and at the bottom of the world's oceans [15]. Industrial exploitation of the deposits of gas hydrates will not only make it necessary to find a number of complicated technological solutions; it will undoubtedly cause enormous and grave ecological problems. The solution of all these problems requires a fundamental knowledge of the thermodynamics of the water–gas system, the kinetics of formation (decomposition) of gas hydrates and their structure. One of the first questions to be answered by researchers studying such unstable objects as gas hydrates concerns areas of thermodynamic stability of certain hydrates (i.e. data on their P, T, X phase diagrams) and any correlation between the stability of hydrates and their structure. The study of clathrate formation at high (up to 10 kbar) pressures in systems where the guest is a liquid that is either soluble in water or hydrophobic (i.e. where hydrates with the stoichiometry 1 : 17 form at moderate pressure [6]) revealed that the 'pressure' parameter is highly informative. For instance, it was found that the upper stability limit of such hydrates was a pressure of about 3 kbar, after which the great majority of them changed to hydrates with the stoichiometry approximately equal to 1 : 7 [16] that were most likely of *CS-I* structure [17]. The study of systems in which *CS-I* hydrates are formed under ambient conditions was complicated by the fact that, under such conditions, the guests are gases, and this required more sophisticated equipment. So far we know of only four systems with a gaseous guest (under ambient conditions) studied at pressures up to 3.5–4.0 kbar: those with nitrogen, argon, methane [18,19] and sulfurous gas [20]. Reference [21] describes the study of the compressibility of the xenon hydrate up to 18 000 bar at $-196\ ^{\circ}$C, which is much lower than the melting point of xenon at ambient pressure.

Here we present data on the decomposition of xenon hydrate both in the presence of excess gas and under gas-deficient conditions at pressures up to l5 000 bar and the temperature range from -25 to +100 $^{\circ}$C, i.e. the phase diagram of the Xe–H_2O system.

2. Experimental

2.1. High Pressure Device

2.1.1. *Creating High Pressures*

The device creating pressures up to l5 000 bar is shown in Figure 1. Cell *1* (described in detail in Figure 2), containing the sample under study, was placed vertically (as shown in Figure 2) into the channel of high pressure vessel *2*. The vessel (thermally insulated with foam plastic jacket *3*) was cooled to the required temperature with

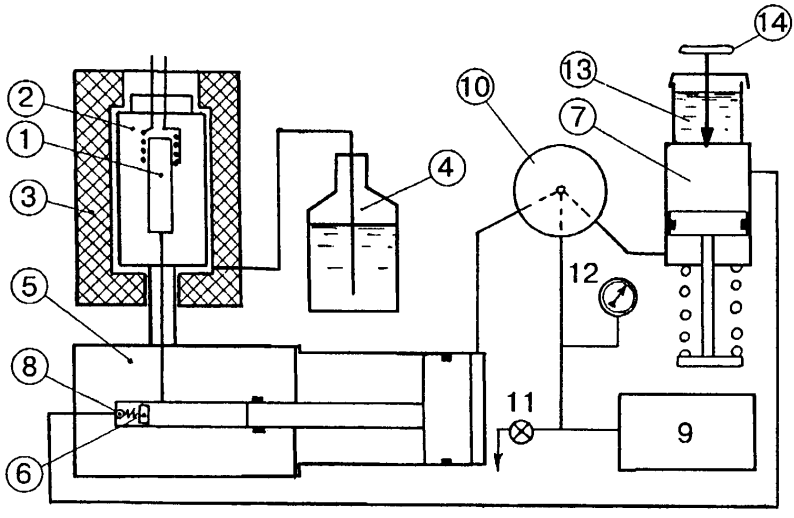

Figure 1. Block diagram of the apparatus for creating pressures up to 15 000 bar for studying the hydrate decomposition (for designations see the text).

liquid nitrogen coming from Dewar flask *4*. A pressure up to 15 000 bar was created with a booster *5* and measured with manganin manometer *6*. A preliminary pressure up to 2000 bar was delivered into the booster from separator *7* through a back valve *8*. Low pressure was created with a three-piston pump *9* and was delivered through distributor *10* either into the low pressure cylinder of the booster or into the separator. Discharge tap *11* makes it possible to decrease pressure. A 2500 bar manometer *12* measures pressure created by the pump. The packing of the booster stem and high pressure compounds was effected by auto tightening. A mixture of polysiloxane oil and benzine in the proportion 1 : 3 was used as a working liquid. It was poured into container *13* and by means of tap *14* was pumped into the separator while its piston was moved down by a spring. Transformer oil was used as a low pressure liquid.

2.1.2. *Cell for Experiments with a Gaseous Component under Pressure*

The drawing of the cell in which measurements were done is presented in Figure 2. The gas under study was pumped into a stainless steel flask *1* of volume about 6 mL at a pressure up to 20 bar. The flask was connected with a caprolon container (0.05 mL) *4* situated inside a copper block *3*. The container was filled with a powder of an inert substance *5* (see below), into which about 0.02–0.03 g of water was introduced. Before that volume *1* was flushed twice with xenon under a pressure of about 10 bar. A thermocouple *6* was introduced into the container through a packing system made of rubber and epoxy compound. The packing of the container was brought about by pressing it with a plate spring *7* against a thin rubber ring *8*. The

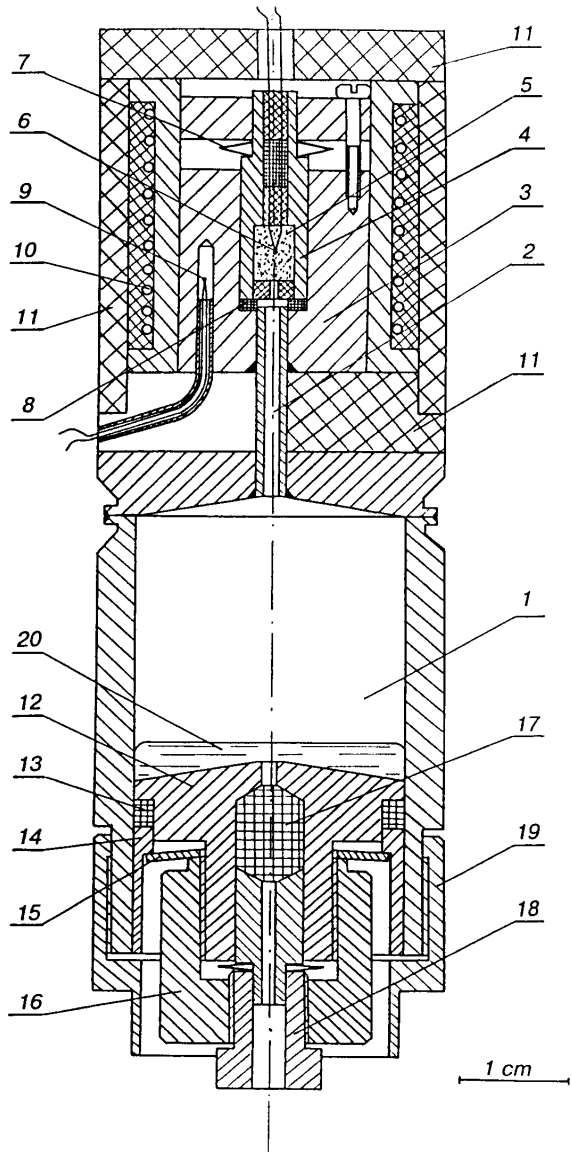

Figure 2. Design of the cell for studying the hydrate decomposition at high pressures (for designations see the text).

standard thermocouple *9* was placed into a specially designed pocket of the copper block *3*. Heating was carried out by means of an electrical resistance furnace *10* isolated from the surrounding medium with fluoroplastic elements *11*. The whole of the cell was placed into the region of high hydrostatic pressure produced by a compressor (Figure 1). The pressure was transmitted into the cell through piston

12 packed with a rubber ring *13*. The initial packing of the ring with an element *14* and a flat spring *15* was achieved with the help of screw *16*. The filling of the cell with the gas was carried out through a hypodermic needle of 0.8 mm diameter introduced into the flask *1* along the channel in the piston *12*, through rubber padding *17*, packed with bolt *18*. A complex-shaped screw *19* prevented the movement of the piston from the flask *1*, which might be caused by the initial gas pressure. Some mercury was poured into the cell to prevent leakage of the gas through the rubber bushings *13* and *17* and to displace the gas into the reaction volume of the container *4* when pressure was exerted.

2.2. MEASUREMENTS AND REAGENTS

The melting (decomposition) points of the forming phases were measured with a chromel–alumel thermocouple (whose characteristic is practically pressure independent in the range considered [22]) by the DTA technique. The thermocouple was calibrated at atmospheric pressure against reference points or a standard thermometer. The reproducibility of temperature measurements within one experimental series was 0.3°, and in a different series it was 1°. Pressure was measured with Bourdon manometers (up to 250 and 2500 bar) calibrated against a load-piston manometer. The accuracy of pressure measurements was 0.5%. At pressures up to 15 000 bar a manganin manometer was used which was calibrated against the melting of mercury [23]. The error in the measurements did not exceed 1%.

To speed up the dissolution of gases, in several cases a nonionogenic surface active substance (SAS) was added, at a concentration in the solution studied of the order of 0.25%. Even though SAS retards the first stage of hydrate formation, i.e., the stage of nucleus formation, it essentially speeds up crystal growth on the nuclei, which ultimately results in about a tenfold acceleration of the reaction studied [24] (previously it was shown that such amounts of SAS did not shift the equilibrium in our accuracy range [25]). To increase the contact surface of water and gas, 0.015–0.025 mL of water was added to an inert substance (powder of SiO_2 and SiC with a grain size of the order of 0.01 cm and filter paper) in the container *4*. The inertness of those substances is confirmed by agreement between the melting curves of the ices and reference data on the one hand and identical results on the hydrate decomposition obtained with different fillers on the other. We used doubly distilled water and xenon of 99.99% purity.

The preparation of a mixture of definite composition in the cell described above is rather difficult because of the possible water loss during the washing of the cell with xenon, which is not taken into account. However, we managed to prepare mixtures with an excess (up to 60-fold, which could be assumed from the volume, the initial pressure in the gas vessel at a certain temperature, and the amount of the water taken) or deficiency of the gas (about 0.6–0.8 with respect to the limiting composition of the hydrate[2]) with ease and reliability. It is clear that to obtain an unambiguous answer to the question about clathrate formation in the system under

Table I. Pressure dependence of the melting points of the xenon eutectic (equilibrium hgs, for designations see Figure 3)

P bar	T°C	P bar	T°C
4260	24.7	5480	58.5
4790	40.8	5610	61.4
4930	43.2	5910	71.5
5020	47.0	6240	80.0
5200	51.2	6290	81.2
5440	58.4	6410	83.4

these experimental conditions (and considering the low mutual solubility of the initial components) is possible only if under the same P, T conditions the number of the hydrates formed in the system does not exceed two. We believe that the latter rule refers to water systems with such simple guests. At least, we do not know of any examples where this is not the case.

3. Results

3.1. Equilibria determined by xenon melting

In the presence of excess xenon the heating curves always showed endothermic effects whose dependence on pressure is illustrated in Figure 3 and Table I. The figure also shows the xenon melting line based on published data [26]. These results indicate that the effects we observed are typical of equilibria accompanying the melting of xenon, and their closeness to the melting points of pure xenon at certain pressures points to low solubility of the hydrate (at temperatures below 78.2 °C, see Section 3.2) and water (at higher temperatures) in the xenon fluid phase.

3.2. Decomposition of the hydrate into aqueous solution and fluid rich in xenon

3.2.1. *Studies with Excess of Xenon*

At ambient pressures xenon forms a hydrate of cubic structure **I** [6, 27, 28]. Its decomposition temperature increases rapidly with pressure from 0 °C at 1.545 bar [28] (1.2 bar according to [1] and 1.52 bar according to [6].) to 35 °C at 60 bar, then it continues to rise less rapidly to 77.8° at 6000 bar (Figure 4, Table II). The hydrate decomposition curve crosses the lines of the three-phase equilibria *hgs* (designations see in Figure 3) and *lgs* (see Section 3.1) in the quadruple point Q_m(*lhgs*).

During the first recording, the heating curve sometimes showed endothermic effects at temperatures close to the melting points of ice modifications correspond-

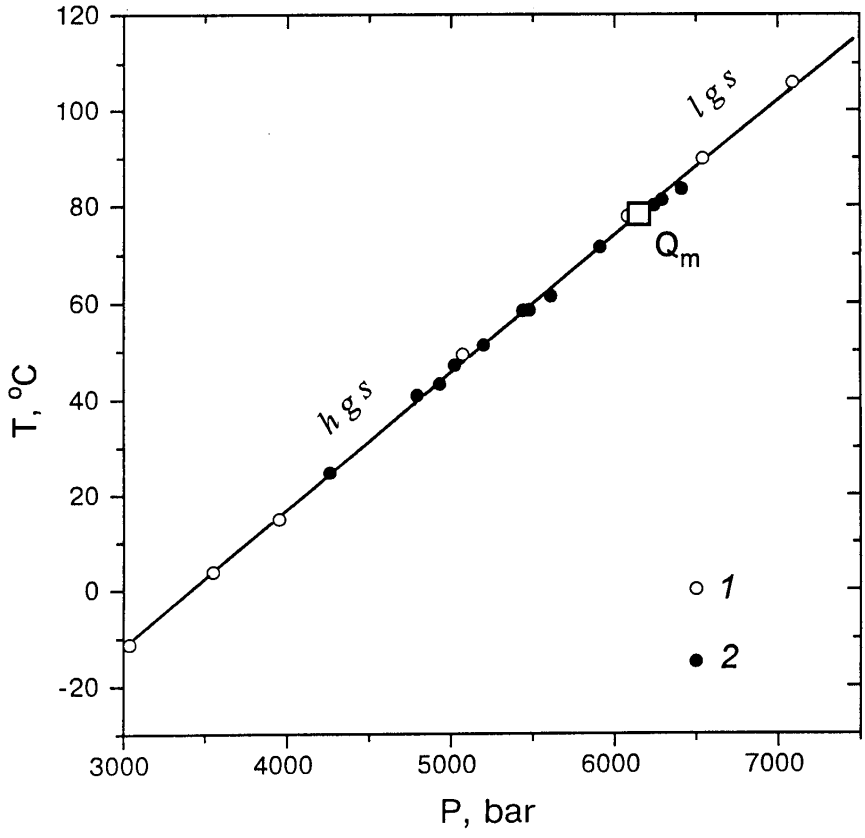

Figure 3. Pressure dependence of xenon melting points (*1*, [20]) and that of the eutectic rich in xenon melting points (*2*, our data) in the xenon–water system. i_k is ice of k modification; l is a liquid phase rich in water; g is gaseous (fluid) phase rich in xenon; s is solid xenon. Q_m is quadruple point $lhgs$. Here and everywhere phases are arranged in order of increasing xenon content.

ing to a certain pressure. However, these effects were not observed when the recording was repeated. This indicated that by that time the clathrate formation reaction was incomplete and the effects were due to the unreacted water.

3.2.2. *Study under Xenon-Deficient Conditions*

As is clear from Figure 4, the data on the decomposition of the hydrate obtained under gas-deficient conditions within the experimental error fall well on the curve obtained with the excess of xenon. However, under these conditions the melting effects of water eutectics are stable (the equilibrium $i_k lh$, where i_k is ice of k modification). We have not given these eutectic equilibria (Figure 5) in detail. They were of interest as a means of checking whether there was a deficiency of xenon during the experiment. As expected, under these experimental conditions it

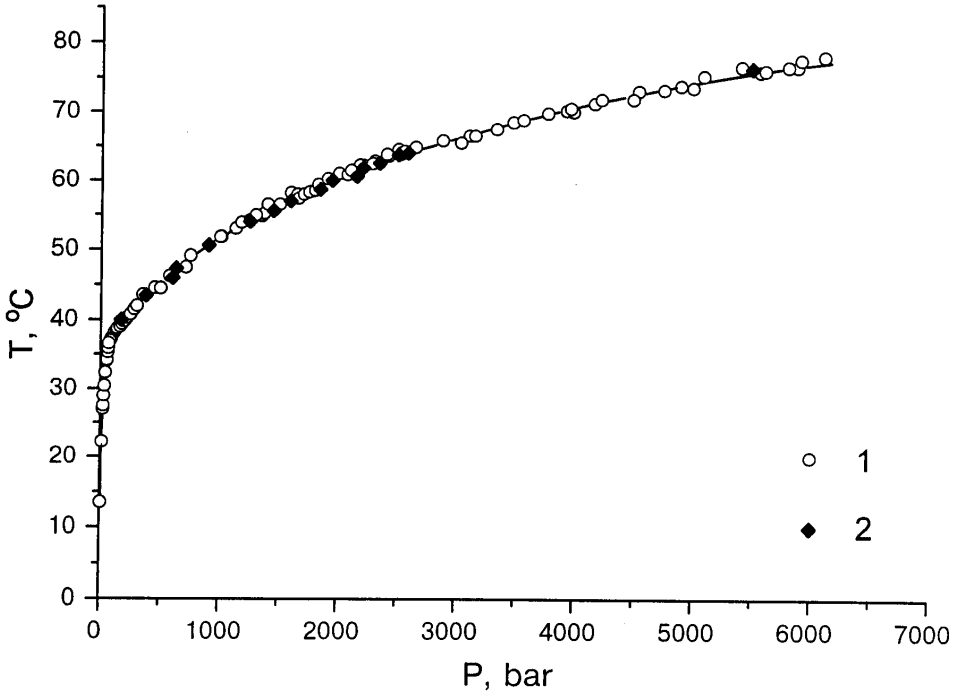

Figure 4. Pressure dependence of the xenon hydrate decomposition points with excess of xenon (1) and under xenon-deficient conditions (2).

is not possible to observe the melting effects of the eutectics rich in xenon (hgs) when equilibrium is achieved. The coincidence of the decomposition curves of the hydrate when the gas is in excess and when there is a deficiency of the gas indicates that in the temperature (and pressure) range under study one hydrate is formed, identical to that forming at ambient pressure, i.e. a *CS-I* hydrate [6].

3.3. DECOMPOSITION OF THE HYDRATE INTO AQUEOUS SOLUTION AND SOLID XENON

The hydrate decomposition curve displays a noticeable break at a pressure of about 6150 bar (Figure 6). Taking account of the data of Section 3.1 we can connect this with the appearance of solid xenon among the decomposition products of the hydrate instead of the fluid phase. The hydrate decomposition points experimental data in the pressure range from 6300 to 15 000 bar are given Table III and Figure 6. The results obtained both with the excess and deficiency of xenon coincide, within the limits of our experimental error.

Table II. Pressure dependence of the temperatures of the xenon hydrate (h) decomposition into liquid (l) and gas-fluid (g) phases (equilibrium lhg).

Excess of xenon						Xenon-deficient conditions	
P bar	T°C	P bar	T°C	P bar	T°C	P bar	T°C
6.75	13.5	1130	53.0	3080	67.0	170	40.0
17.8	22.2	1180	53.9	3100	66.5	375	43.5
23.8	27.0	1250	54.2	3150	66.5	600	46.0
26.8	27.5	1300	54.9	3330	67.5	630	47.3
30.6	29.0	1370	55.2	3470	68.5	900	50.6
35.6	30.4	1400	56.5	3554	68.8	1250	54.0
40.6	32.3	1500	56.5	3762	69.8	1450	55.6
51.0	34.0	1593	58.2	3920	70.2	1590	57.0
54.0	34.2	1650	58.0	3956	70.5	1840	58.7
61.0	35.3	1705	58.0	3980	70.0	1950	60.0
66.0	35.9	1750	58.3	4090	71.5	2150	60.6
69.0	36.6	1800	58.5	4157	71.2	2200	61.8
78.0	37.0	1825	59.4	4217	71.8	2340	62.5
86.2	37.2	1906	60.2	4485	71.8	2500	63.7
90.6	37.4	2000	61.0	4530	73.0	2580	64.0
112	38.1	2070	60.8	4745	73.2	5490	76.3
134	38.6	2100	61.4	4880	72.8		
139	38.8	2160	61.7	4887	73.8		
162	39.0	2174	62.2	4980	74.5		
177	39.4	2200	62.2	4990	73.5		
200	39.8	2280	62.4	5030	73.5		
219	40.3	2300	62.8	5066	74.8		
250	40.8	2340	62.5	5230	75.0		
280	41.5	2400	63.8	5297	75.0		
300	42.0	2413	63.5	5400	75.5		
350	43.6	2500	64.5	5480	76.0		
450	44.6	2517	63.8	5558	75.8		
500	44.5	2550	64.2	5600	76.0		
575	46.2	2644	64.8	5796	76.5		
750	49.1	2875	65.8	5871	76.5		
1000	51.8	3030	65.5	6000	77.8		

4. Discussion

4.1. PHASE DIAGRAM

The above data allow us to draw the P, T projection of the phase diagram of the water–xenon system (Figure 7). Let us consider the phase equilibria around the quadruple point $Q_m(lhgs)$. Four lines of monovariant (three-phase) equilibria

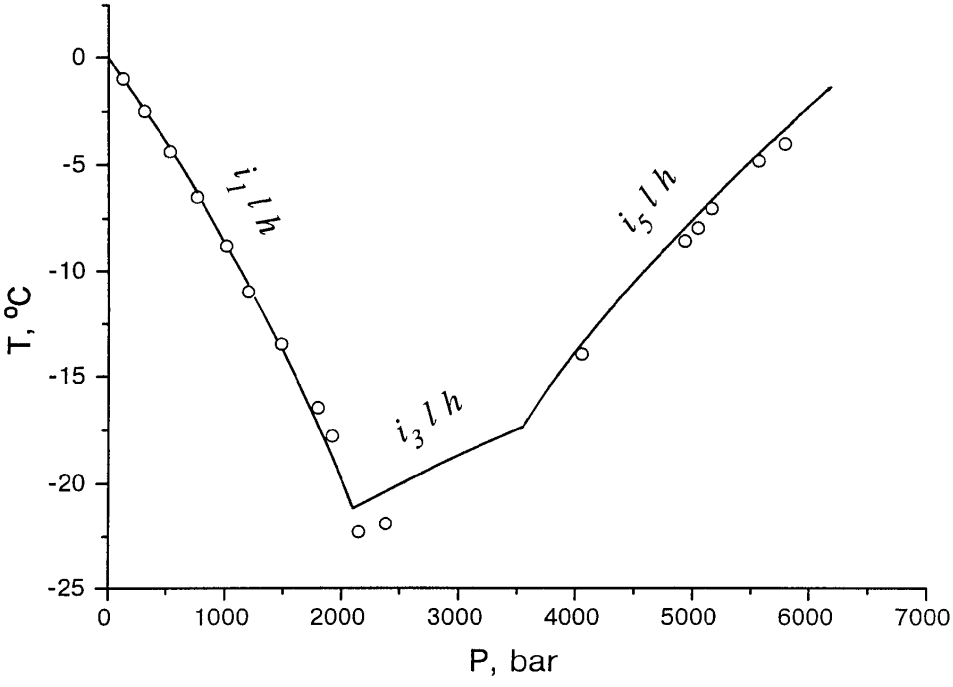

Figure 5. Pressure dependence of the eutectic rich in water in the xenon-water system (open circles) in comparison with the ice melting points (solid lines).

Table III. Pressure dependence of the temperatures of the xenon hydrate (h) decomposition into liquid (l) and solid xenon (s) phases (equilibrium lhs).

P bar	T°C	P bar	T°C	P bar	T°C	P bar	T°C
6300	78.5	8750	78.7	10700	77.5	13550	70.7
6450	78.5	8800	79.5	10800	76.7	13770	70.1
6600	78.7	9000	79.2	11000	75.9	13900	70.0
6840	79.0	9200	79.5	11330	75.6	14000	69.8
7000	79.2	9370	78.5	11620	74.9	14080	69.4
7250	79.2	9500	79.0	12000	75.3	14200	70.0
7300	79.5	9650	78.2	12300	74.1	14250	69.0
7500	79.5	9700	77.8	12500	73.0	14450	68.7
7600	79.1	9800	78.8	12700	72.7	14630	67.7
7800	79.6	10000	77.5	12900	72.4	14750	67.8
8000	79.5	10000	78.5	13000	71.8	14900	68.0
8200	79.5	10160	77.2	13250	71.2	15000	67.0
8500	79.5	10250	78.1	13400	71.3	15000	66.7

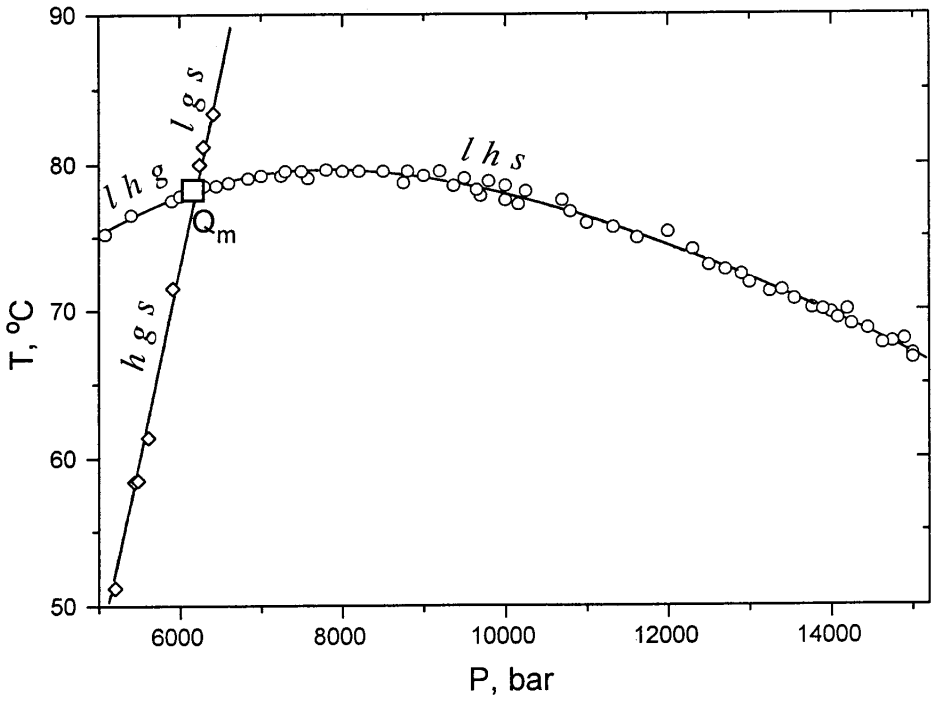

Figure 6. The curve of the xenon hydrate decomposition into water solution and solid xenon (lhs), four-phase equilibrium $Q_m(lhgs)$ and its environment.

emerge from this point (as from each quadruple point of the binary system), dividing the field into six bivariant (two-phase) parts. Three crystallization fields with the hydrate are situated in the temperature ranges bounded from above (along the temperature axis) by the lines of the monovariant equilibria lhg and lhs. Under xenon-deficient conditions (with respect to the hydrate composition) the whole of this space to the lines $i_k lh$ belongs to the bivariant field lh. In the range of temperatures bounded by the lines $i_k lh$ the liquid water phase l disappears, to be replaced by the ice i_k modification corresponding to the pressure, i.e. the bivariant equilibria $i_k h$ exist under these conditions. Since xenon is not soluble in ices and only slightly soluble in liquid water, on the P, T projection these fields essentially coincide with the crystallization fields of the ices, while the fields of crystallization of ices from water xenon solutions ($i_k l$) are degenerate.

With excess xenon two more bivariant fields with the hydrates hg and hs situated between the lines $lhg - hgs$ and $hgs - lhs$, respectively, adjoin the point Q_m. Obviously, under these conditions in the temperature and pressure range under study these fields are not limited from below.

Two out of the three remaining bivariant fields, without hydrate phases (lg, ls), adjoining the point Q_m are found at temperatures above the stability range of the hydrate indicated by the lines lhg and lhs. A portion of the third field (gs) is below

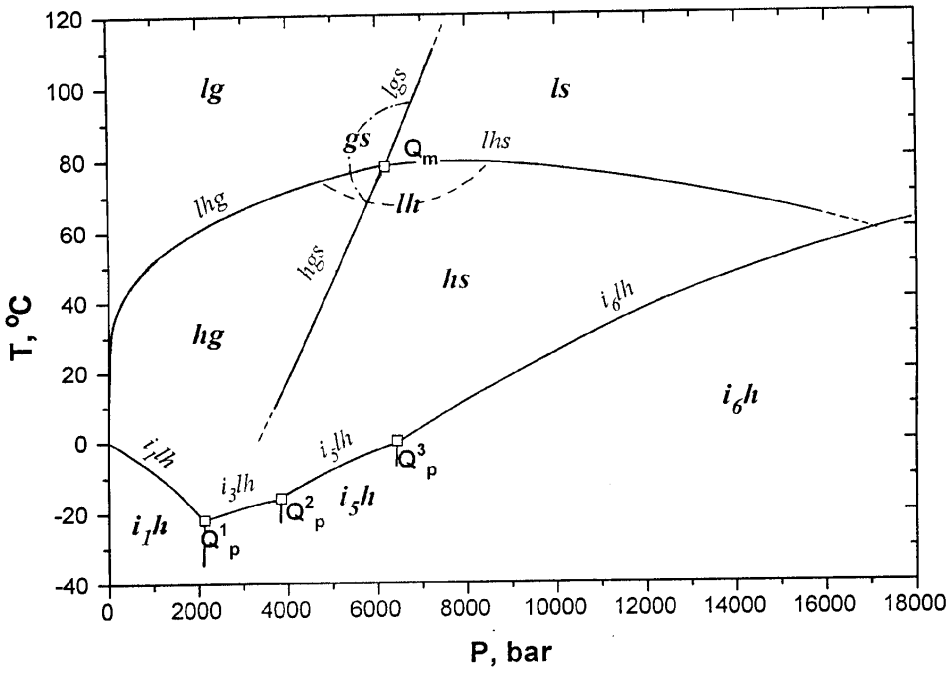

Figure 7. P, T Projection of the phase diagram of the xenon–water system. Q_m is quadruple point $lhgs$; Q_p^1 (and so on) is quadruple point $i_1 i_3 lh$ (for other designations see Figure 3).

the lines lhg, and the hydrate instability here is due to low concentration (low partial pressure) of water.

4.2. Structure and stability

Our review [16] includes a comprehensive discussion of the interrelation between the structure of hydrates and their stability under pressure. As might be expected, there is an apparent correlation between the packing coefficients of the hydrates changing widely (from 0.47 to 0.59) and their stability to pressure (dt/dp of the melting or decomposition of the hydrates into substances in a condensed state varies from -3.8 to +10 K/kbar). In a general case wide variations in the packing coefficients of the hydrates are due to the fact that, in the case of many water frameworks, it is enough to fill only the so-called 'large' cavities for the structure to be stabilized. Therefore, since the ratio of the small to the large cavities varies widely (e.g., from 2 for *CS-II* to 0.33 for *CS-I*), the packing coefficient of the hydrate structures with vacant small cavities varies significantly. However, if both types of cavities are occupied by the guest molecules, the difference in the packing coefficients between various structures becomes negligible, and the packing coefficients approach the upper limit indicated above.

In xenon hydrates even at low pressures (1.545 bar) the degree of filling of the large (y_l) and small cavities (y_s) is quite high and equals $y_l = 0.980$ and $y_s = 0.716$ [27,28]. The dimensions and the shape of a xenon molecule, like those of some other molecules, fit well both the large and the small cavities of the *CS-I* framework. This results in rather a high (for clathrate hydrates) packing coefficient: $k = 0.564$ [16][3] even under ordinary conditions. At high pressures the filling degree of both types of cavities might be expected to approach unity; hence $k = 0.581$.

The rather high ability of xenon to undergo a dispersion interaction explains an extremely high (for gas hydrates) decomposition temperature of xenon hydrate (78.2 °C at 6150 bar). However, since the compressibility of xenon is rather high (with pressure increase from 1 to 6150 bar along the melting line the volume of the fluid phase decreases by 13.5%, that of the solid phase by 6.4% although temperature rises from $-111\,7^{\circ}$ to 78.2 °C [26]), the volume of the decomposition products of the hydrate (i.e. the volume of the water and fluid phase) at 6000 bar becomes essentially equal to that of the hydrate. As a result of a step decrease of the molar volume of xenon (by 6% [26]) during transformation of the latter from the fluid to the solid state the volume of the decomposition products of the hydrate (i.e. the volume of the water phase and solid xenon) becomes practically equal to that of the hydrate, and at pressures up to 6150–9500 bar the decomposition temperature is practically independent of pressure. At higher pressures, due to a greater compressibility of the decomposition products, their volume becomes smaller than that of the hydrate, and with pressure increase the decomposition curve goes down slowly along the temperature axis, reaching 67 °C at 15 000 bar. If higher pressure does not result in another denser hydrate, the decomposition curve of the hydrate might be expected to cross the melting curve of the water eutectic (which essentially coincide with the melting curve of ice VI due to the relatively low solubility of xenon in water) at a pressure of about 17 kbar, after which the curve of the hydrate decomposition into solid xenon and ice VI will decline even more steeply because transformation of the water phase into ice VI is accompanied by a step decrease of the volume. Therefore, we can expect the existence of the upper stability limit for the classic *CS-I* gas hydrates, which should be situated below that of xenon hydrate because the latter is one from the most stable and well packing hydrates of this structure.

It can be seen that throughout the pressure and temperature range we studied under ambient pressure the *CS-I* xenon hydrate does not undergo any phase transition. A similar picture was observed at l8 000 bar and −196 °C [21]. Thus, it can be predicted with reasonable certainty that in the water–xenon system, one *CS-I* hydrate forms in this pressure range and the temperature range from −196 °C to the decomposition temperature, as distinct from the water systems with argon [31] and krypton [32], in which case three hydrates were discovered in the same pressure range. This shows that *CS-II* are less compact structures than *CS-I* hydrates, even in the case where both types of cavities are fully occupied.

Acknowledgments

The authors are grateful to the International Science Foundation (Grants RBR 000 and RBR 300) for making this work possible and to N. Udachina for translating this paper into English.

Notes

[1] It was believed [6] that all guest molecules of size less than 5.2–5.4 Å formed *CS-I* hydrates, guest molecules of size 5.8–7 Å formed *CS-II* hydrates, and guest molecules of intermediate size could stabilize both structures [8], while molecules whose dimensions exceed the above values did not form hydrates at all. It was shown [7] that small molecules, as has already been mentioned (Ar, Kr, O_2, N_2), stabilized *CS-II* hydrates, and very large molecules, like methylcyclohexane, stabilized the so-called 'H-structure' (or *HS-III*), provided an auxiliary gas (such as H_2S, for example) was present [9].

[2] When all types of cavities are filled by the same kind of guests, the hydrate number is within the range 5.67–5.75 for the most typical frameworks of gas hydrate type [16].

[3] The packing coefficient $k = \Sigma\nu_i/V$, where $\Sigma\nu_i$ is the total volume of the molecules constituting a phase with the volume V [29]. To calculate it we used the following reference values: van der Waals radii of oxygen $R_0 = 1.29$ Å, hydrogen $R_H = 1.16$ Å, xenon $R_{\mathrm{Xe}} = 2.18$ Å [30], $a = 11.97$ Å [6], the length of the H bond $l_H = 2.80$ Å. Based on these initial data, the volume occupied by a water molecule in the hydrate $\nu_{\mathrm{H_2O}} = 14.12$ Å^3 [16], and the volume of a xenon atom $\nu_{\mathrm{Xe}} = 43.40$ Å^3.

References

1. C.R. Forcrand: *C. R. Acad. Sci.* **181**, 15 (1925).
2. C.R. Forcrand: *C. R. Acad. Sci.* **176**, 355 (1923).
3. M. Godchot, G. Cauquil, and R. Calas: *C. R. Acad. Sci.* **202**, 759 (1936).
4. B.A. Nikitin: *Z. Anorg. Allg. Chem.* **227**, 81 (1936).
5. M. Villard: *C.R. Acad. Sci.* **123**, 377 (1896).
6. M. Stackelberg and H.R. Muller: *Z. Elektrochem.* **58**, 25 (1954).
7. D.W. Davidson, S.K. Garg, S.R. Gough, Y.P. Handa, C.I. Ratcliffe, J.S. Tse, and J.A. Ripmeester: *J. Incl. Phenom.* **2**, 231 (1984).
8. D.R. Hafemann and S.L. MilIer: *J. Phys. Chem.* **73**, 1392, 1398 (1969).
9. J.A. Ripmeester, J.S. Tse, C.I. Ratcliffe, and B.M. Powell: *Nature* **325**, 135 (1987).
10. D. Londono, W.F. Kuhs, and J.L. Finney: *Nature* **332**, 141 (1988); *J. Chem. Phys.* **97**, 547 (1992).
11. Yu.A. Dyadin: in *Crystallography of Supramolecular Compounds*, Eds. G. Tsoucaris, J.L. Atwood, and J. Lipkowski: NATO ASI Series C, Vol. 480, p. 223 (1995).
12. W. Vos, L. Finger, R. Hemley, and Ho-kwang Mao: *Phys. Rev. Lett.* **71**, 3150 (1993).
13. Yu.A. Dyadin and E.Ya. Aladko: *J. Incl. Phenom.* **20**, 115 (1995).
14. V.G. Vasil'ev, Yu.F. Makogon, A.F. Trebin, A. Trofimuk, and N.V. Cherski: The Property of Natural Gases that Occur in the Earth's Crust in the Solid State, '*Otkrytia izobretenia i tovaryne znaki*' (*Discoveries, Inventions and Commercial Licence Signs*), N 10, 4 (1970).
15. K.V. Kvenvolden: in *International Conference on Natural Gas Hydrates*, E.D. Sloan, J. Happel, and M.A. Hnatow (eds.), *Ann. N-Y. Acad. of Sci.* **715**, 232 (1994).
16. Yu. A. Dyadin, I.V. Bondaryuk, and F.V. Zhurko: *Inclusion Compounds*, J.L. Atwood, J.E.D. Davies, and D.D. MacNicol (eds.), Oxford University Press, Oxford, Vol. 5, 213 (1991).
17. M. Zakrzewski, D.D. Klug, and J.A. Ripmeester: *J. Incl. Phenom.* **17**, 237 (1994).
18. S.H. Saito, D.R. Marschall, and R. Kobayashi: *AIChEJ.* **10**, 734 (1964).
19. D.R. Marschall, S.H. Saito, and R. Kobayashi: *AIChEJ.* **10**, 22 (1964).
20. J.G. van Berkum and G.A. Diepen: *J. Chem. Thermodynamics* **11**, 317 (1979).
21. Y.P. Handa, J.S. Tse, D.D. Klug, and E. Whalley: *J. Chem. Phys.* **94**, 623 (1991).
22. D.S. Tsiklis: *Physico-Chemical Techniques for Investigations under High and Superhigh Pressures*, M. 'Khimiya', p. 198 (Russian) (1976).

23. V.S. Bogdanov and A.P. Miroshnikov: *Trudy metrologicheskikh institutov SSSR.* M. 'Izd-vo standartov, vyp. 104, 33 (1969).
24. O.B. Kutergin, V.P. Melnikov, and A.N. Nesterov: *Doklady RAN* **323**, 549 (1992).
25. Yu.A. Dyadin, F.V. Zhurko, and T.V. Mikina: *Izvestia SO AN SSSR*, Ser. khim. nauk, vyp. 4, 65 (1988), *Chem. Abstr.*, **109**, 157373r (1988).
26. P.H. Lahr and W.G. Eversole: *J. Chem. Eng. Data* **7**, 42 (1992).
27. M.J. Collins, C.I. Ratcliffe, and J.A. Ripmeester: *J. Phys. Chem.* **94**, 157 (1990).
28. D.W. Davidson, Y.P. Handa, and J.A. Ripmeester: *J. Phys. Chem.* **90**, 6549 (1986).
29. A.I. Kitaigorodski: *Molekuliarnye Kristally*, Nauka, Moskva (1971).
30. Yu.V. Zefirov and P.M. Zorkij: *Uspekhi khimii* **58**, 713 (1989).
31. Yu.A. Dyadin, E.G. Larionov, D.S. Mirinski, T.V. Mikina, and L.I. Starostina: *Mendeleev Commun.*, No. 1, **32**, 1997.
32. Yu.A. Dyadin, E.G. Larionov, D.S. Mirinski, T.V. Mikina, E.Ya. Aladko, and L.I. Starostina: *Proceedings of 2nd Conference of Natural Gas Hydrates*, Toulouse, June 2–6, p. 59 (1996).